

Original Article

ATP7A as a prognostic biomarker and potential therapeutic target in gastric cancer

Zhongmei Shi^{1,2}, Zhiyun Mao¹, Ming Cui¹, Dongjin Xu², Yan Wang³, Rongrong Jing¹

¹Department of Laboratory Medicine, Affiliated Hospital of Nantong University, Medical School of Nantong University, Nantong 226001, Jiangsu, China; ²Department of Laboratory Medicine, Dongtai Hospital of Traditional Chinese Medicine, Dongtai 224200, Jiangsu, China; ³Department of Pathology, Affiliated Hospital of Nantong University, Nantong 226001, Jiangsu, China

Received November 7, 2024; Accepted December 20, 2024; Epub January 15, 2025; Published January 30, 2025

Abstract: Objectives: To investigate the roles of Cu transporter ATPase copper transporting alpha (ATP7A) in gastric cancer (GC) progression and prognosis. Methods: ATP7A expression was investigated using databases, immunohistochemistry (IHC) and qPCR in tumor tissues and GC cell lines. Diagnostic and prognostic value of ATP7A was assessed by Receiver Operating Characteristic (ROC) and Kaplan-Meier curve, respectively. The roles of ATP7A were explored using protein-protein interaction (PPI), Gene Ontology (GO), Kyoto Encyclopedia of Genes and Genomes (KEGG) and Gene Set Enrichment Analysis (GSEA), ssGSEA algorithm and Tumor Immune Estimation Resource (TIMER) databases. Subsequently, the effects of ATP7A were evaluated by Cell Counting Kit-8 (CCK-8), colony formation, and transwell assays. Results: ATP7A overexpression was associated with a higher IHC score and a larger area under the ROC curve (0.746). Elevated ATP7A expression correlated with shorter survival time, greater invasion depth of GC lesions, advanced pathological stages, and older age in GC patients. Comprehensive analysis revealed that ATP7A was involved in copper ion transport, transition metal ion homeostasis, cellular transition metal ion homeostasis, and copper ion homeostasis. Additionally, ATP7A was linked to key signaling pathways, including Hedgehog, Wnt/ β -catenin, and Notch, along with the top 10 hub genes. Furthermore, ATP7A played a role in immune infiltration, influencing T cells, dendritic cells, B cells, macrophages, and neutrophils, as well as the expression of immune checkpoints such as Cytotoxic T-Lymphocyte-Associated Protein 4 (CTLA-4), Programmed Cell Death Protein 1 Ligand 1 (PD-L1), T-Cell Immunoglobulin, and Mucin Domain-Containing Protein 3 (TIM-3). Experimental validation demonstrated that silencing ATP7A suppressed GC cell proliferation, colony formation, migration, and invasion. Conclusion: ATP7A promoted GC progression and acted as a promising prognostic target for the treatment of GC.

Keywords: Gastric cancer, ATP7A, cell proliferation, cell migration, cell invasion

Introduction

Gastric cancer (GC) is one of the most prevalent malignancies worldwide. According to global cancer statistics, 968,000 new cases of GC and 660,000 deaths were reported in 2022 [1]. Due to the subtle symptoms of early-stage GC, most patients are diagnosed at advanced stages. Unfortunately, despite standard treatments such as surgery, chemotherapy, and radiotherapy, the 5-year survival rate for advanced GC remains only 36.2% [2]. In recent years, promising new approaches, including immunotherapy, have been explored for GC patients [3]. However, due to the complexity of the tumor

immune microenvironment, there is a lack of reliable biomarkers for accurate diagnosis and management to effectively guide immunotherapy in GC. Therefore, the urgent identification of novel molecular targets is critical to improving the diagnosis and treatment of GC.

Copper is a redox-active metal ion essential for maintaining human homeostasis. In 2022, Tsvetkov et al. identified a novel pattern of cell death termed *cuproptosis*, which is induced by copper and associated with mitochondrial respiration [4]. Unlike other known forms of cell death, cuproptosis relies on the intracellular accumulation of copper ions. These ions bind

directly to lipoylated enzymes, disrupting the tricarboxylic acid (TCA) cycle, leading to the aggregation and dysregulation of TCA cycle proteins, ultimately triggering cell death. Cuproptosis has been implicated in various cancers [5-7]. This discovery opens new avenues for the prevention and treatment of GC. In our study, we identified 19 cuproptosis-related genes, including ATPase copper transporting alpha (ATP7A) [4, 8]. ATP7A, localized in the cellular Golgi apparatus, is a P-type ATPase enzyme responsible for heavy metal transport [9]. Beyond its role in copper transmembrane transport, ATP7A plays a critical role in cancer pathogenesis [10]. Notably, ATP7A enhances tumor invasiveness by supplying large quantities of copper ions to oncogenic enzymes across various tumor types [11, 12]. However, the role of ATP7A in the clinical characteristics of GC and its impact on patient prognosis remain unclear.

The primary objective of this study is to investigate the expression pattern, clinical significance, and biological functions of ATP7A in GC. We aim to determine whether ATP7A can serve as a prognostic biomarker and a potential therapeutic target for GC patients. Meanwhile, the functional regulations of ATP7A were examined through a series of comprehensive analyses, including Gene Ontology (GO), protein-protein interaction (PPI), Kyoto Encyclopedia of Genes and Genomes (KEGG), Gene Set Enrichment Analysis (GSEA), and Tumor Immune Estimation Resource (TIMER) databases. Furthermore, the roles of ATP7A in GC cell growth, migration, and invasion were verified through *in vitro* experiments, with the hope of providing a reference for future GC research and clinical treatment. The research flowchart is shown in **Figure 1**.

Materials and methods

Data acquisition and preprocessing

Data acquisition and preprocessing: All pan-cancer data, including tumor samples from various cancer types ($n = 18,102$), were obtained from the UCSC Xena website (<https://xenabrowser.net/datapages/>). This comprehensive dataset facilitated a broad analysis of gene expression patterns across different malignancies. Differentially expressed gene data were derived from RNA-seq information in *The Cancer Genome Atlas* (TCGA)-Stomach Adenocarcinoma (STAD) project in level 3 HTSeq-

Counts format [13]. The series matrix file of GSE54129 was retrieved from the Gene Expression Omnibus database. Notably, RNA-seq data in FPKM format were converted to Transcripts Per Million (TPM) format and subjected to \log_2 transformation for further analysis.

Tissue samples

Two GC tissue microarrays (ZL-stmA961 and ZL-stmA962) were obtained from Shanghai Wellbio Technology Co., Ltd. (Shanghai, China). Additionally, the tissue microarray (Hstm-A180su20) was provided by Shanghai Outdo Biotech Company. The final analysis included 152 GC tissues and 117 adjacent healthy tissues.

Data for 375 gastric cancer tumor samples and 32 healthy tissues were extracted from *The Cancer Genome Atlas* (TCGA) database, a comprehensive resource offering a vast collection of molecular data on various cancer types. These samples were instrumental in analyzing ATP7A expression levels and their correlation with clinical outcomes. Utilizing TCGA data enabled a robust and comprehensive evaluation of ATP7A's role in gastric cancer. Student's *t*-test was employed to compare ATP7A expression levels between different groups.

Cell lines and cultivation

Homo sapiens gastric cancer cell lines (HGC-27, MKN-45, AGS, and MKN-74) and epithelial cells (GES-1) were obtained from the Shanghai Cell Bank (Chinese Academy of Sciences, China). The cells were cultured in RPMI-1640 medium. The MGC-803 cell line was purchased from Hanhong Biotechnology (Nanjing) Co., Ltd. and maintained in DMEM high-glucose medium at 37 °C with 5% CO₂.

Small interfering RNA (siRNA) transfection

SiRNA specific for ATP7A and a non-specific control were provided by Hanhong Biotechnology Co., Ltd. (Nanjing) and transfected using G073 RNAiFectin™ transfection reagent (Abcam, CA) according to the manufacturer's protocol, when cells reached 30-40% confluency. Six hours after transfection, the medium containing the transfection reagents was replaced with fresh medium. Cells were harvested 48 hours post-transfection. The siRNA sequences

ATP7A in gastric cancer: biomarker and therapeutic target

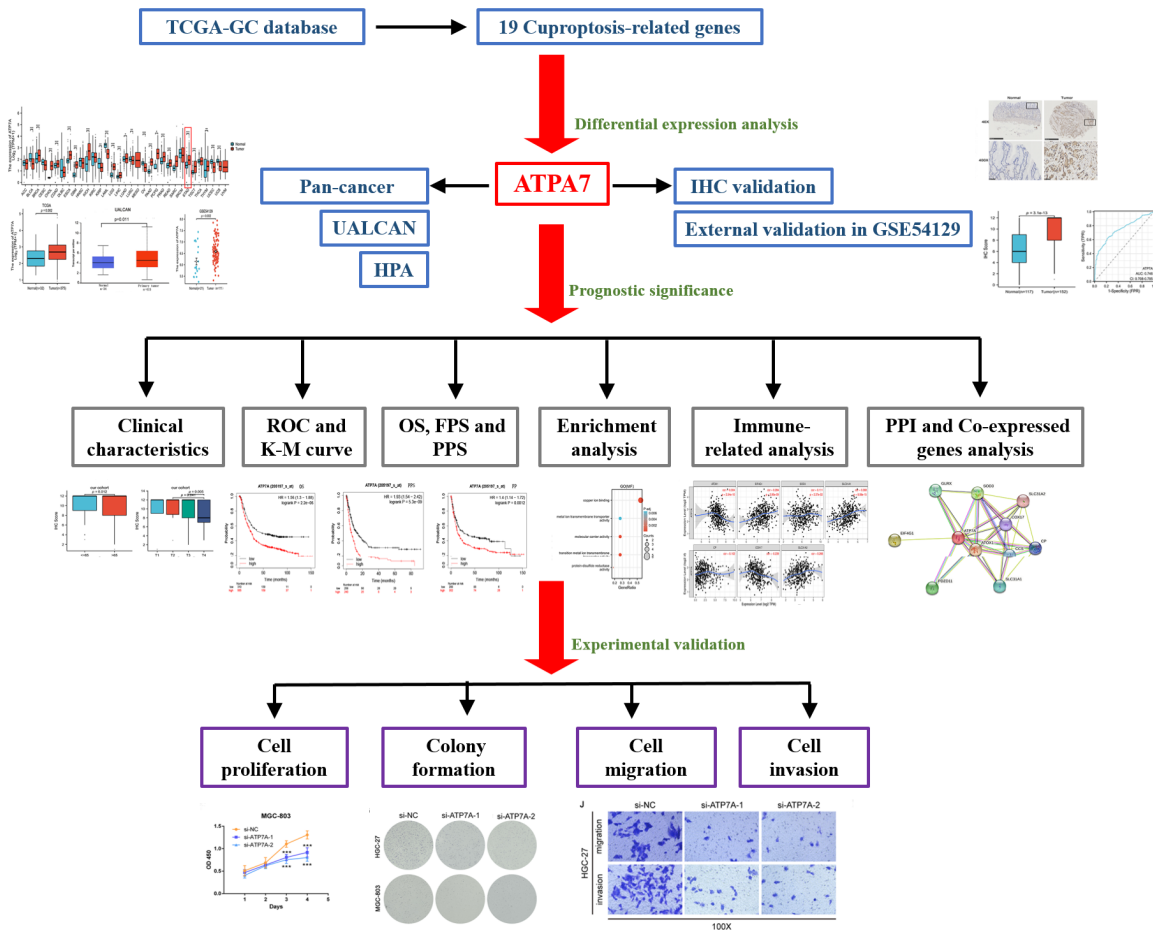


Figure 1. The research flow chart. TCGA-GC: The Cancer Genome Atlas - Gastric Cancer; ROC: Receiver Operating Characteristic; K-M curve: Kaplan-Meier curve; OS: Overall Survival; FPS: Five-Year Progression-Free Survival; PPS: Progression-Free Survival; HPA: Human Protein Atlas; IHC: Immunohistochemistry; PPI: Protein-Protein Interaction.

are described as follows: ATP7A (homo) siRNA-1-3040: 5'-AGGUAAAGGUAGUGGUUUTT; ATP7A (homo) siRNA-2-3538: 5'-UGACUGAACAU-GAGAGAAATT; Si-NC sense: 5'-UUCUCCGAACG-UGUCACGUTT.

Total RNA extraction and qPCR

The Facture® Cell/Tissue Total RNA Isolation Kit V2 was used to extract total RNA. After confirming the RNA concentration and purity, reverse transcription into cDNA was performed using the reverse transcription kit. All reagent kits were obtained from Vazyme Biotech Co., Ltd. (Nanjing, China). The cDNA was then diluted 10 times for subsequent experiments. PCR was performed with the following conditions: denaturation at 95°C for 15 s, annealing at 60°C for 10 s, extension at 72°C for 40 s,

and 42 cycles. The primer sequences are described below: GAPDH-F: 5'-GCACCGTCAA-GGCTGAGAAC; GAPDH-R: 5'-TGGTGAAGACGCC-AGTGGA; ATP7A-F: 5'-CCCTCTAGGAACAGCCAT-AACC; ATP7A-R: 5'-ATACCACAGCCTGGCACAA-CCT.

qPCR was performed using SYBR Green (Applied Biosystems) on an ABI Q7 Pro Sequence Detection System (Applied Biosystems). The expression of ATP7A was calculated using the $2^{-\Delta\Delta CT}$ method.

Western blot

RIPA lysis buffer (Strong) (GLPBIO, USA) was used to extract protein from GC cells. Sample proteins were separated by 6% sodium dodecyl sulfate polyacrylamide gel electrophoresis

ATP7A in gastric cancer: biomarker and therapeutic target

(SDS-PAGE) (Biosharp, China) and transferred to polyvinylidene fluoride membranes (Millipore, Bedford, MA). The membranes were incubated with ATP7A antibody (PA7106, 1:1000, Abmart, China), followed by incubation with a secondary antibody (goat anti-rabbit, ZB2301, ZSBio, China). Antibodies against GAPDH (#60004-1-Ig, 1:5000, Proteintech, USA) were used as controls. The membrane was then exposed using the Ultra High Sensitivity ECL Kit (GLPBIO, USA).

Cell Counting Kit-8 (CCK-8) assay

For each sample, 100 μ L of transfected cell suspension was placed into 96-well plates and incubated overnight at 37°C. After settling, 10 μ L of CCK-8 reagent (ab228554, Abcam, USA) was added and incubated for an additional hour at 37°C. The absorbance was measured at 450 nm using a microplate reader (EPOCH2, BioTek).

Colony formation assay

Cell suspension (1000 cells/well) was seeded into a 6-well plate and cultured continuously at 37°C with 5% CO₂ for two weeks. Colony growth was monitored, and the medium was changed as necessary. Afterward, colonies were fixed with 1% methanol for 15 minutes, washed with PBS, and stained with 0.1% crystal violet (C0121, Beyotime Biotechnology, China) for 10 minutes. The dye was gently washed off with tap water, and the colonies were allowed to air dry. Finally, the colonies were photographed and counted.

Transwell assay

The transwell assay was performed to evaluate the migration and invasion capabilities of GC cells. For the migration assay, transfected cells were seeded into the upper chamber with serum-free medium, while the bottom chamber contained medium with 10% serum. For the invasion assay, diluted matrix gel was coated onto the upper chamber. After 48 hours of incubation, the invasive cells were stained with crystal violet (C0121, Beyotime Biotechnology, China) and photographed under a microscope (IX73, Olympus, Japan).

Immunohistochemically (IHC) staining and evaluation

The experimental process was as follows: (1) The tissue chips were baked in a 60°C incubator for 2 hours, then soaked in xylene twice for 10 min each time. (2) The chips were placed in different concentrations of ethanol (100%, 95%, 80%, and 75%), followed by distilled water, for 5 min each at room temperature (RT). (3) The chips were washed three times with PBS buffer for 5 min each, then treated with an endogenous peroxidase inhibitor for 10 min at RT. This was followed by a 30-min blocking step with 10% goat serum at RT. (4) The tissue sections were incubated overnight with diluted primary antibodies (ATP7A, 1:200, PA7106, Abmart, China) at 4°C. Afterward, a 30-min incubation with a labeled secondary antibody (goat anti-rabbit, 1:50, A0208, Beyotime, China) was performed at RT. (5) The sections were washed with PBS and then developed with DAB. Hematoxylin was used for counterstaining. (6) The sections were photographed under a microscope. Five random fields were selected, and the percentage of positively stained tumor cells was evaluated relative to the whole tumor area, with scores assigned as follows: 0 for 0%, 1 for 1-25%, 2 for 26-50%, 3 for 51-75%, and 4 for 76-100%. (7) The staining intensity was scored on a scale of 0-3: 0 for no staining, 1 for pale yellow, 2 for brownish yellow, and 3 for tan.

The IHC-score is defined as the positive area ratio score \times staining intensity score [14].

Comprehensive data analysis

The expression of ATP7A in GC was predicted using TCGA (GSE54129) and the UALCAN database (<http://ualcan.path.uab.edu/index.html>) [15]. Specifically, protein expression was assessed using the Human Protein Atlas (<https://www.proteinatlas.org/>) [16]. STRING (<https://cn.string-db.org/>) [17] was used to search for co-expressed genes and construct PPI networks. TIMER (<https://cistrome.shinyapps.io/timer/>) [18] was used to verify the correlation between ATP7A and co-expressed genes. The GO (<https://david.ncifcrf.gov/>) and KEGG (<https://www.kegg.jp/>) [19] databases were utilized to explore the functions of ATP7A and the associated pathways, using default param-

eters: $p\text{-adjust} < 0.05$, $|\log_2FC| \geq 1$, analyzed with DESeq2 software. GSEA [20] was performed using the “ClusterProfiler” package, with over 5,000 genome alignments for each analysis. The h.all.v7.2.symbols.gmt file from MSigDB (<https://www.gsea-msigdb.org/gsea/msigdb/index.jsp>) database [21] was used for comparison. The modified P -value and false discovery rate were both set to < 0.05 , with absolute normalized enrichment scores ($|NES|$) > 1 considered significant. The TIMER database (<http://timer.cistrome.org/>) was used to examine the expression of ATP7A in the immune microenvironment. Additionally, the score of 24 infiltrating immune cells was calculated using the ssGSEA algorithm based on the “GSVA” package [22]. Gene sets for immune cells were provided by past literature [23]. The relationship between ATP7A expression and immune regulatory genes was examined using the TIMER “Correlation” module. The connection between ATP7A expression and immune checkpoints was confirmed with the GEPIA (<http://gepia.cancer-pku.cn/>) database [24].

Protein expression analysis

To complement our mRNA expression data, we utilized the Human Protein Atlas (HPA) database (<https://www.proteinatlas.org/>), which provides a valuable resource for tissue-based protein expression data. The HPA database was used to compare protein levels of ATP7A in normal human gastric tissues and gastric cancer tissues. This allowed us to gain insights into the protein expression patterns of ATP7A and correlate these with our mRNA data, providing a more comprehensive understanding of ATP7A's role in gastric cancer.

Statistical analysis

We used R software (v.4.2.1) and GraphPad Prism 8.0 (Chicago, CA) for statistical analysis. The expression differences of ATP7A were assessed using Student's t -test among groups. Kaplan-Meier (K-M) [25] survival curves were plotted, and the Chi-square test was used to evaluate the relationship between ATP7A and patient characteristics. Overall survival (OS), post-progression survival (PPS), and progression-free survival (PFS) based on ATP7A expression were estimated using the Cox regression hazards model. The “Receiver Operating Characteristic (pROC)” package [26] was used

to plot the ROC curve for differentiation verification. Spearman correlation analysis was applied to assess the correlation between gene expressions. A P -value < 0.05 was considered statistically significant.

Results

Screening of cuproptosis-related gene

Nineteen cuproptosis-related genes were identified through literature review, including FDX1, SLC31A1, PDHB, PDHA1, NFE2L2, GCSH, MTF1, LIPT1, LIPT2, NLRP3, LIAS, GLS, DLD, DLST, DBT, DLAT, CDKN2A, ATP7A, and ATP7B. By comparing the expression of these genes between 375 GC tumor samples and 32 healthy tissues, 13 significantly differentially expressed genes were identified. Subsequently, 11 prognostic genes were confirmed in GC patients ($P < 0.05$). According to the existing literature, three hub genes had not been evaluated in GC, particularly ATP7A, which plays a critical role in copper homeostasis by transferring copper ions from cells to extracellular spaces (as shown in **Figure 2**). Therefore, we selected ATP7A as our study subject.

ATP7A expression and diagnostic value in GC

To assess the diagnostic value of ATP7A in GC, a pan-cancer database was screened. We found that ATP7A expression was increased in 16 out of the total 33 tumors, especially in tumors of the digestive system (**Figure 3A**). Further analysis of ATP7A expression in GC through the TCGA database revealed that ATP7A was significantly upregulated in GC tissues compared to adjacent healthy tissues (**Figure 3B**). Similarly, ATP7A expression was also elevated in GC in the UALCAN database (**Figure 3C**). For verification, we used the GSE54129 dataset to evaluate ATP7A expression in GC, confirming that ATP7A was significantly higher in GC tumors compared to non-cancer tissues (**Figure 3D**). Additionally, the HPA database was searched to compare ATP7A protein levels in normal gastric tissues and GC tissues. The results showed that a large number of positive particles were present in GC tissues, mainly localized in the cytoplasm or cell membrane (**Figure 3E**). To further validate ATP7A levels, we performed IHC staining, which showed stronger ATP7A expression in GC tumors compared to gastric epithelial tissues

ATP7A in gastric cancer: biomarker and therapeutic target

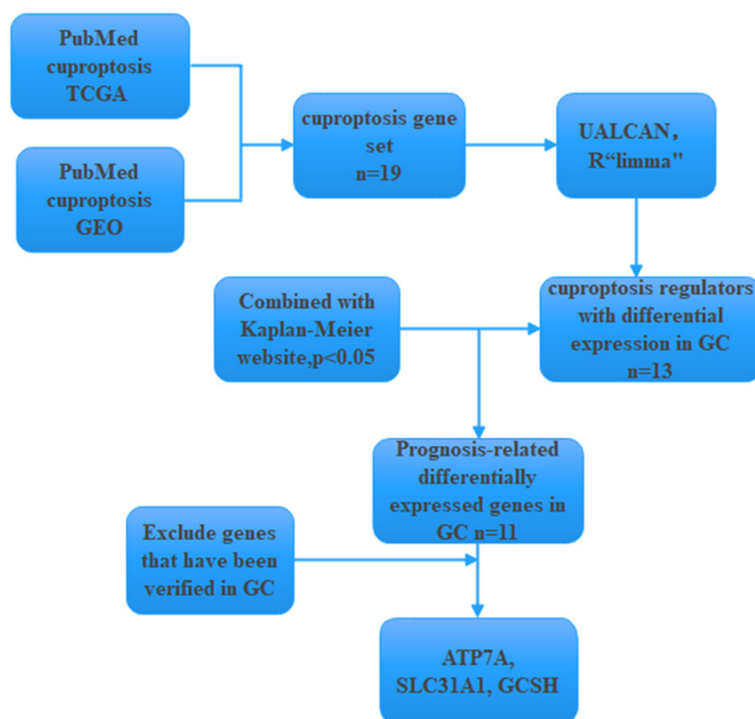


Figure 2. The process of hub gene screening. TCGA: The Cancer Genome Atlas; GEO: Gene Expression Omnibus; GC: Gastric Cancer; ATP7A: ATPase copper transporting alpha; SLC31A1: Solute Carrier Family 31 Member 1; GCSH: Glycine Cleavage System H Protein.

(**Figure 3F**). The staining score analysis indicated altered expression of ATP7A in GC (**Figure 3G**). The diagnostic profile of ATP7A in GC was also analyzed through the ROC curve, with the area under the curve being 0.746 (**Figure 3H**). These findings suggest that ATP7A has excellent diagnostic efficacy in GC.

Prognostic potential of ATP7A in GC

To evaluate the prognostic relevance of ATP7A in GC patients, we utilized the TCGA database to examine the connection between ATP7A expression and corresponding clinical data. Based on the TCGA database, ATP7A expression was correlated with the T phase ($P < 0.05$), N phase, and pathological stage ($P < 0.001$) (**Figure 4A-F**). Additionally, our experimental data showed that ATP7A expression was correlated with the T phase ($P = 0.005$) and the age of GC patients ($P = 0.012$) (**Figure 4G, 4H**). Overall, overexpression of ATP7A was associated with a worse prognosis in GC.

To further visualize the survival differences between high and low expression groups of

ATP7A, Kaplan-Meier (K-M) survival curves were applied, as shown in **Figure 5A-C**. The K-M curve demonstrated a significant decline in OS, PFS, and PPS in the high ATP7A expression group compared to the low expression group. GC patients with higher ATP7A levels exhibited worse OS in subgroups based on pathological stage, T stage, and N stage (**Figure 5D-I**). These findings suggest that ATP7A could serve as a prognostic biomarker for GC patients.

Analysis of functional enrichment of ATP7A in GC

To better understand the roles of ATP7A in GC, potential interactions between ATP7A and other proteins were screened using the STRING database. Ten genes were found to interact with ATP7A, namely ATOX1, EIF4G1, SOD3, PDZD11, GLRX, SLC31A1, CCS, CP, COX17, and SLC31A2 (**Figure 6A**). The interactions of co-expressed genes in GC tissues were further analyzed using TIMER and displayed in **Figure 6B**. It was revealed that ATP7A was positively associated with five co-expressed genes - EIF4G1, SOD3, SLC31A1, CP, and SLC31A2 - but negatively correlated with ATOX1 and COX17 ($P < 0.05$). Additionally, the biological effects of ATP7A were annotated using GO and KEGG enrichment analyses. The most significant enrichment of ATP7A in biological processes included copper ion transport, transition metal ion homeostasis, cellular transition metal ion homeostasis, and copper ion homeostasis. Regarding cellular components, ATP7A was primarily localized in the late endosome, basal plasma membrane, basolateral plasma membrane, and recycling endosomes. In terms of molecular functions, ATP7A was associated with copper ion binding, molecular carrier activity, and transition metal ion transmembrane transporter activity (**Figure 6C**). KEGG enrichment analysis indicated that ATP7A was mainly involved in mineral absorption and platinum drug resistance (**Figure 6D**). Furthermore,

ATP7A in gastric cancer: biomarker and therapeutic target

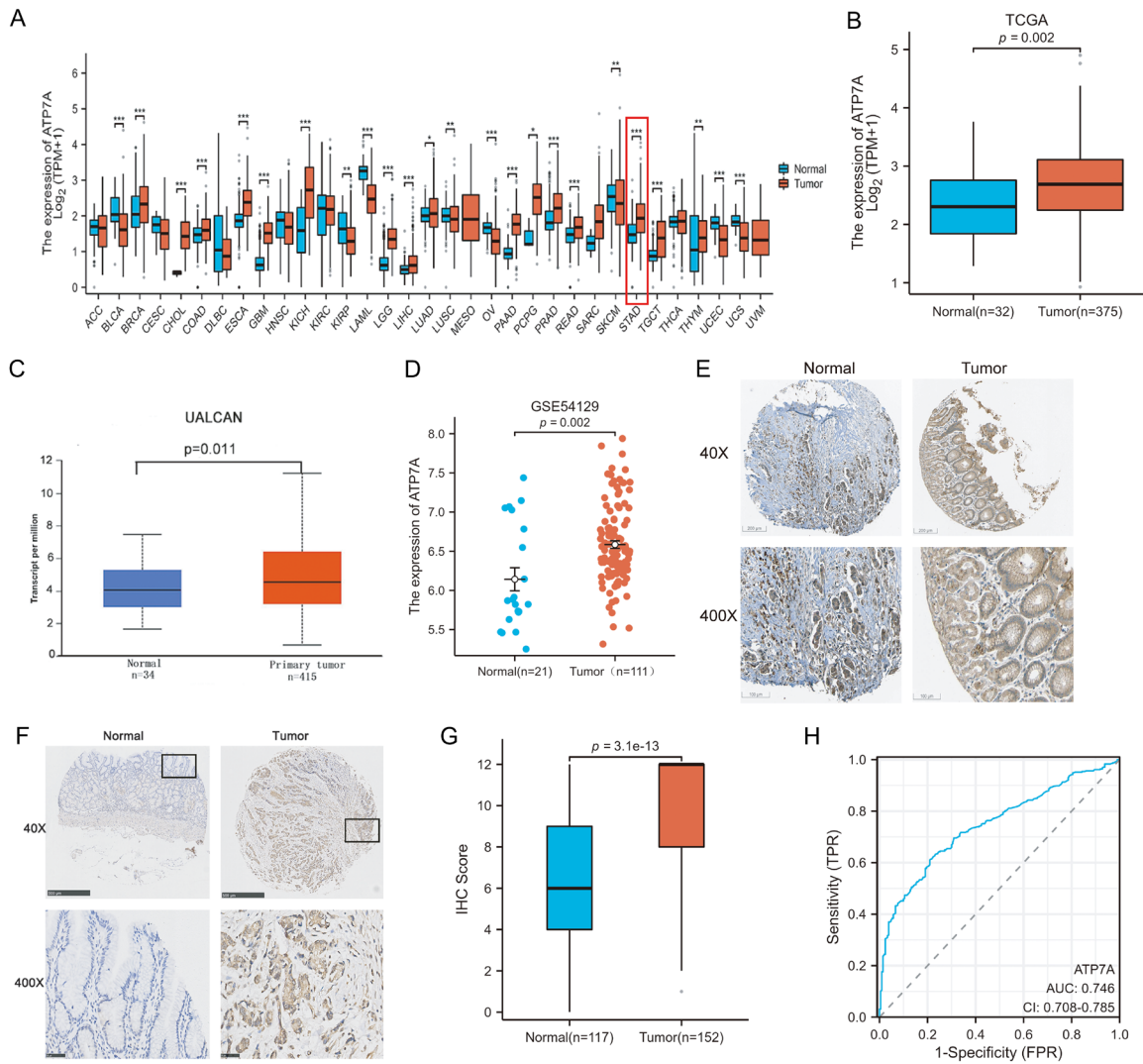


Figure 3. ATP7A expression and diagnostic value in GC. A. ATP7A expression was presented based on Pan-cancer databases. B, C. The differential expression of ATP7A in GC from TCGA and UALCAN database. D. TCGA dataset (GSE54129) showed the high expression of ATP7A in GC tumors. E. HPA database indicated the differences of ATP7A in normal and tumor tissues. F. IHC staining in tumor tissues. G. The IHC score of ATP7A (normal n = 117, tumor n = 152). H. ROC curve of the diagnostic performance of ATP7A in GC. Compared to normal tissues, * $P < 0.05$, ** $P < 0.01$, *** $P < 0.001$ (magnification $\times 40$ and 400 , scale bar = 100 and $200 \mu\text{M}$).

GSEA results showed enrichment in Notch, Hedgehog, and Wnt/ β -catenin signaling pathways (Figure 6E-G). To sum up, these enrichment results suggest that ATP7A may influence the biological processes of GC through various pathways.

Roles of ATP7A in GC immune landscape

Since immunotherapy has achieved unprecedented success in GC, the use of immune checkpoint inhibitors is considered a promising avenue for GC treatment. Therefore, we investi-

gated whether ATP7A expression is related to immune status to guide treatment decisions. The association between ATP7A levels and immune status was explored using the TIMER database. The results indicated a positive correlation between ATP7A and B cells ($P = 1.49\text{e-}04$), CD4+ T cells ($P = 3.23\text{e-}06$), macrophages ($P = 1.34\text{e-}06$), and dendritic cells ($P = 1.76\text{e-}03$) (Figure 7A). Additionally, changes in somatic copy number (SCNA) of ATP7A were linked to the infiltration levels of dendritic cells, T cell subsets (CD8+ and CD4+), B cells, macrophages, and neutrophils (Figure 7B). We ana-

ATP7A in gastric cancer: biomarker and therapeutic target

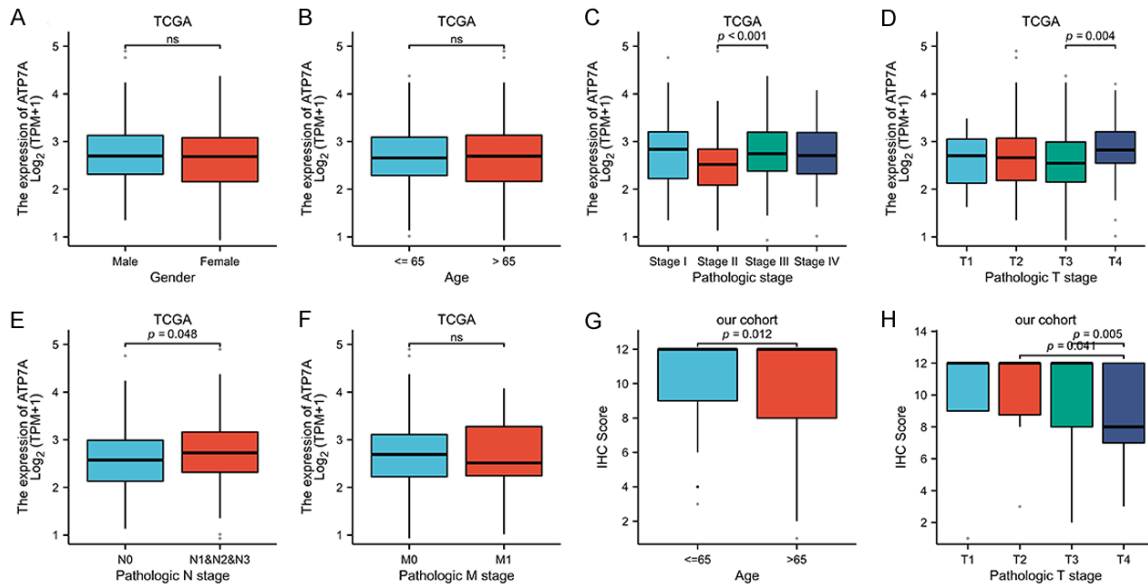


Figure 4. Association between ATP7A and clinical features. (A-F) The relationship between ATP7A and clinical characteristics of patients in TCGA database. ATP7A expression was associated with age (G) and T stage (H) in our cohort. ns: no significance.

lyzed 24 subsets of immune cells in GC tumor immunity, revealing statistical significance in eosinophils, immature dendritic cells, mast cells, macrophages, T helper cells, central memory T (T_{cm}) cells, and effector memory T (T_{em}) cells in the high ATP7A expression groups. In contrast, the low ATP7A expression groups showed higher enrichment scores in plasmacytoid dendritic cells only ($P < 0.05$, **Figure 7C**). Furthermore, surface marker analysis of immune cell subsets revealed a positive association between ATP7A levels and M2 macrophages (CD163, MRC1, IL-10, VISG4, MS4A4A), dendritic cells (CD1C, ITGAX, NRP1, THBD), and M1 macrophages (CD68) (**Figure 7D**). Also, a positive correlation was observed between ATP7A and CD274 (programmed death ligand 1, PD-L1), cytotoxic T lymphocyte antigen 4 (CTLA-4), and HAVCR2 (T cell immunoglobulin and mucin domain-containing protein 3, TIM-3) in GC (**Figure 7E-G**). Consistently, these relationships between ATP7A and immune checkpoints were also evident in the GEPIA database (**Figure 7H-J**). These findings suggest that ATP7A may be involved in immune cell infiltration.

Knocking down ATP7A inhibited GC cell proliferation, colon formation, migration and invasion

Based on the observations above, ATP7A was closely associated with the prognosis of GC. To

evaluate the role of ATP7A in GC malignancy, we measured ATP7A expressions in GC cell lines, and compared them to the normal human gastric mucosal epithelial cell line (GES-1). A significant upregulation of ATP7A was observed in HGC-27 and MGC-803 cell lines ($P < 0.05$) (**Figure 8A**). Consequently, we applied ATP7A siRNA (si-ATP7A-1/-2) in GC cells. The transfection efficacy of si-ATP7A was confirmed, with ATP7A levels significantly reduced in both si-ATP7A-1 and si-ATP7A-2 groups at the mRNA (**Figure 8B**) and protein levels (**Figure 8C** and **8D**) ($P < 0.05$) compared to si-NC groups. CCK-8 assays showed that blocking ATP7A significantly decreased the survival rate of HGC-27 and MGC-803 cells ($P < 0.05$) (**Figure 8E** and **8F**). The colony formation assay demonstrated that si-ATP7A-1/-2 significantly inhibited colony growth in both cell lines (**Figure 8G-I**). Additionally, the migration and invasion capacities were impaired by si-ATP7A-1 and -2 in GC cells (**Figure 8J-O**). Collectively, these findings indicate that ATP7A knockdown exerts a significant inhibitory effect on GC development.

Discussion

In this study, we investigated the role of ATP7A in GC, exploring its diagnostic and prognostic significance, as well as its potential impact on cancer immunotherapy. ATP7A, a transmembrane protein, plays a critical role in maintain-

ATP7A in gastric cancer: biomarker and therapeutic target

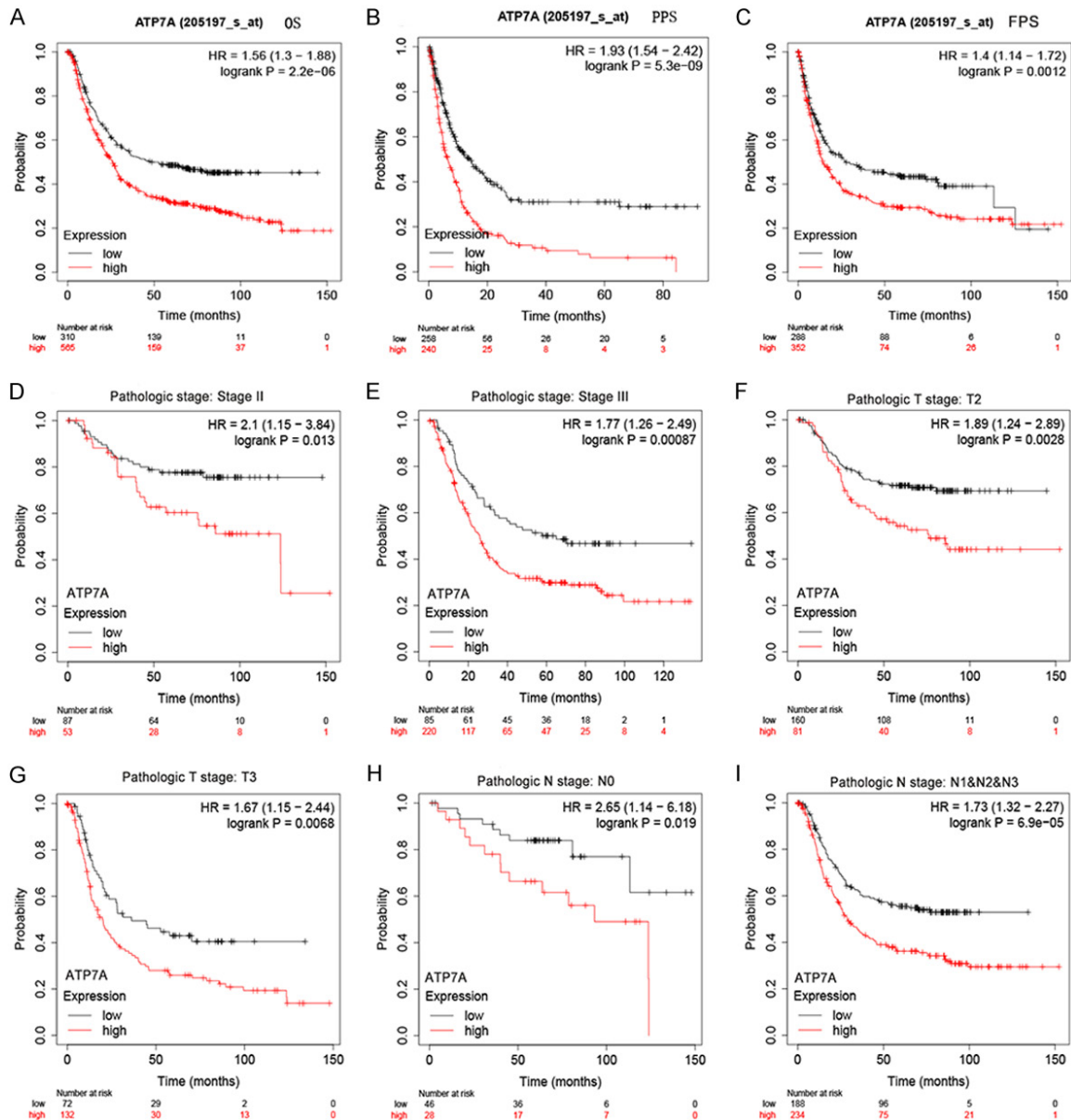


Figure 5. The relation between ATP7A and prognostic factors in GC patients. A-C. K-M survival curves of ATP7A were established to present OS, FPS and PPS using TCGA database. D-I. Overall survival curves depending on high levels of ATP7A in clinical stage T and N.

ing copper homeostasis [27]. Under physiological conditions, when cytosolic copper concentrations are low, ATP7A resides in the trans-Golgi network, where it transfers copper ions to cuproenzymes in the secretory pathway. However, when cytoplasmic copper levels increase, ATP7A moves to the plasma membrane, where it facilitates the export of excess copper ions. Previous studies have demonstrated that altered ATP7A expression can lead to X-linked diseases in infants, children, and adolescents,

including Menkes disease, occipital horn syndrome, and X-linked distal hereditary motor neuropathy [28-30]. Notably, elevated ATP7A expression has been associated with poor outcomes in ovarian and hepatocellular carcinoma [11, 31]. High levels of ATP7A have also been observed in esophageal squamous cell carcinoma, correlating with poorly differentiated tumor tissues [12]. However, the prognostic role of ATP7A in GC has not been fully explored. In our study, we first assessed ATP7A expres-

ATP7A in gastric cancer: biomarker and therapeutic target

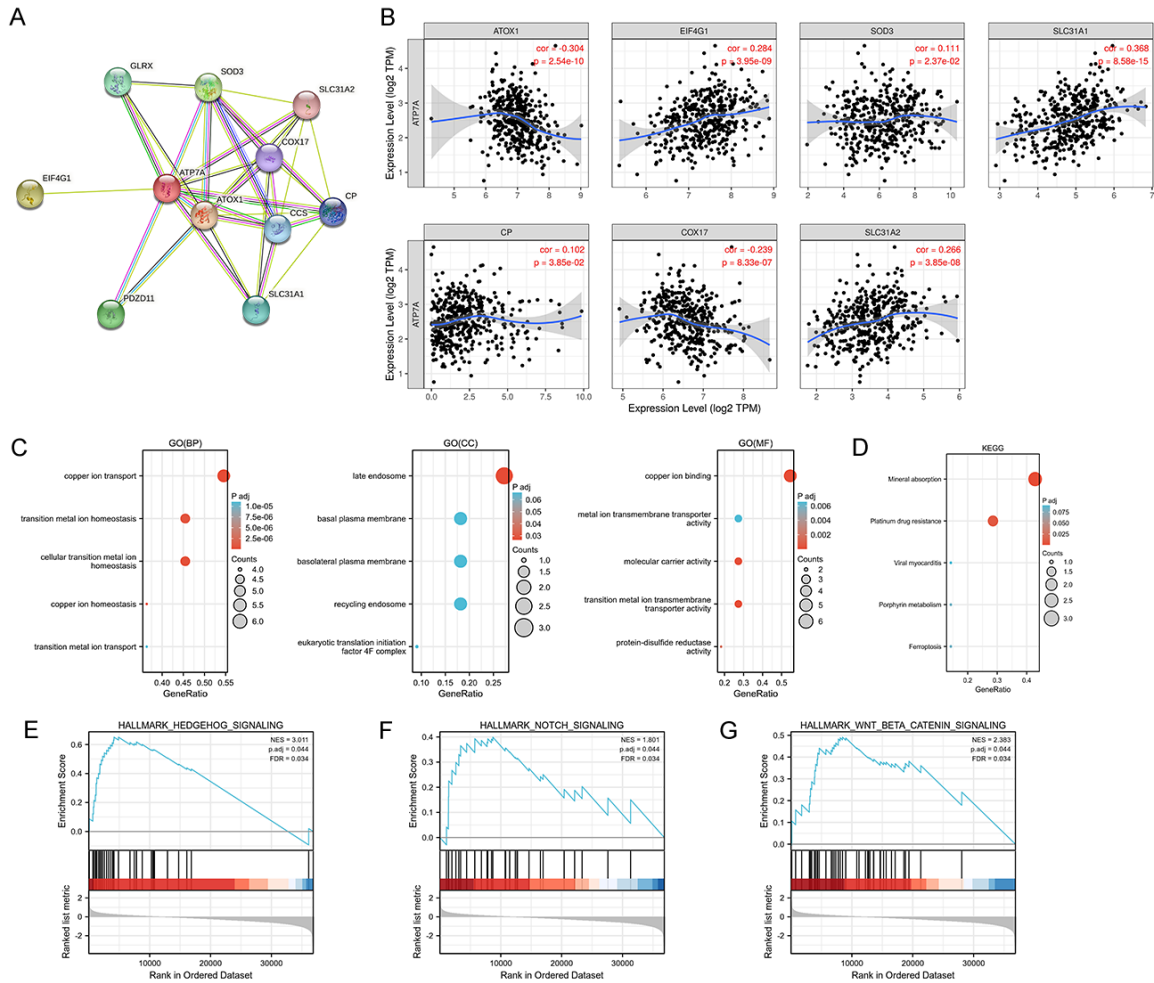


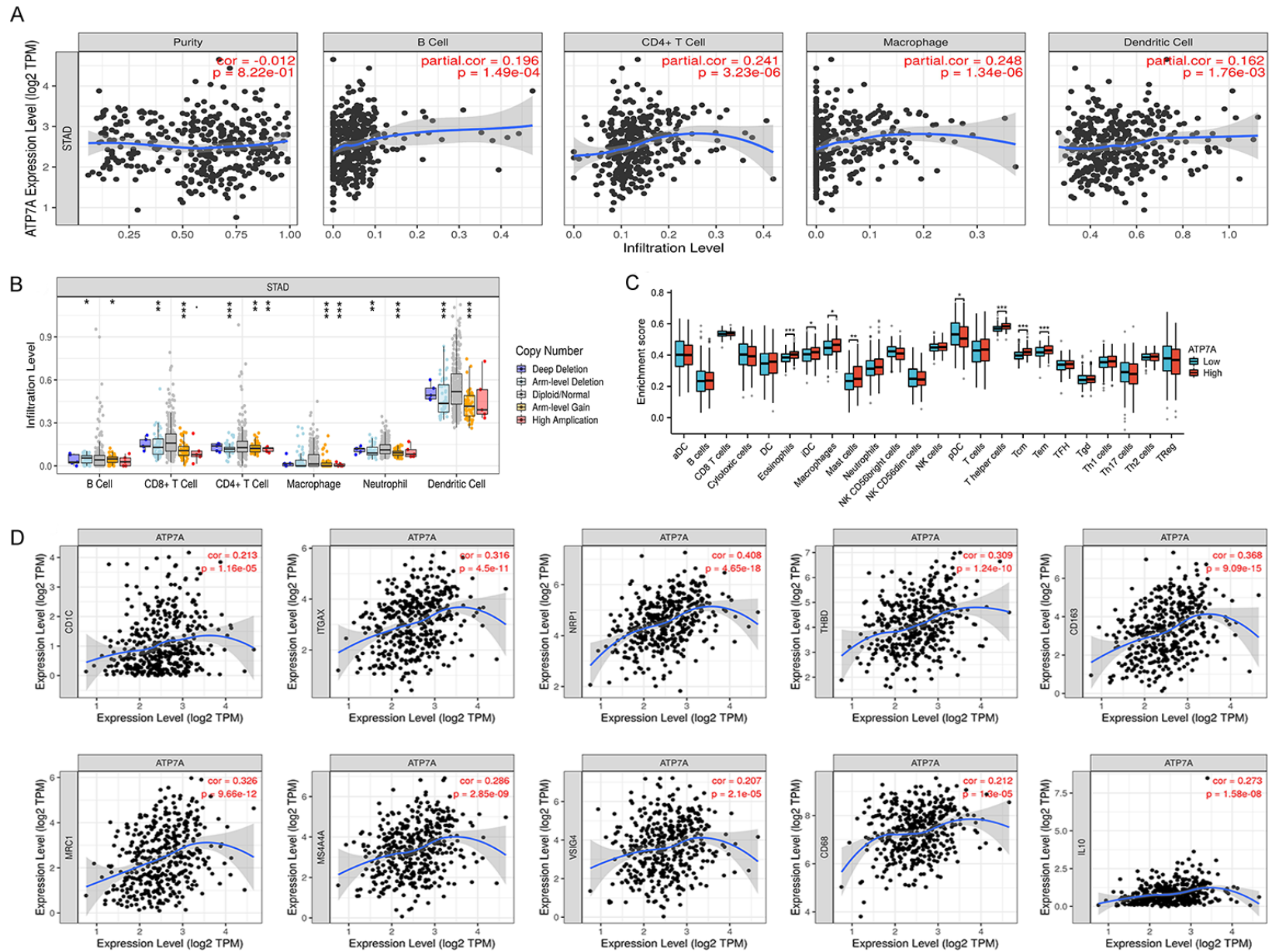
Figure 6. Functional enrichment of ATP7A in GC. A. The PPI network was graphed using STRING. Ten related genes were confirmed to have regulatory relationships. B. TIMER database was used to analyze the correlation of ATP7A with hub genes. C, D. GO and KEGG pathway enrichment analysis of differential expressed genes. E-G. GSEA functional enrichment analysis.

sion in GC tissues using multiple databases, and then validated the findings through IHC and qPCR. Our results demonstrated upregulated ATP7A expression in GC tissues compared to adjacent normal tissues. High ATP7A expression was associated with advanced T and N stages and older age in GC patients. Additionally, patients with higher ATP7A expression showed significantly worse OS, PFS, and PPS. These findings were consistent with our observations that ATP7A was highly expressed in both GC cells and tumor tissues.

To explore the regulatory roles of ATP7A in GC, we conducted a literature review and analyzed various databases. It has been reported that ATP7A is involved in platinum-based drug resis-

tance in tumors, with its expression linked to the prognosis and treatment outcomes of platinum-based chemotherapy [32]. By analyzing KEGG and GO signaling pathways, we found that ATP7A plays a key role in copper ion transport and transition metal ion transmembrane transporter activity, both of which are critical in the platinum resistance pathway. Additionally, GSEA revealed that ATP7A was significantly enriched in the Wnt/ β -catenin, Hedgehog, and Notch signaling pathways. Previous studies have highlighted the crosstalk between the Hedgehog, Notch, and Wnt pathways, which synergistically contribute to tumorigenesis [33]. Since these signaling pathways are involved in various cancer-related processes, including tumor cell proliferation, maintenance of cancer

ATP7A in gastric cancer: biomarker and therapeutic target



ATP7A in gastric cancer: biomarker and therapeutic target

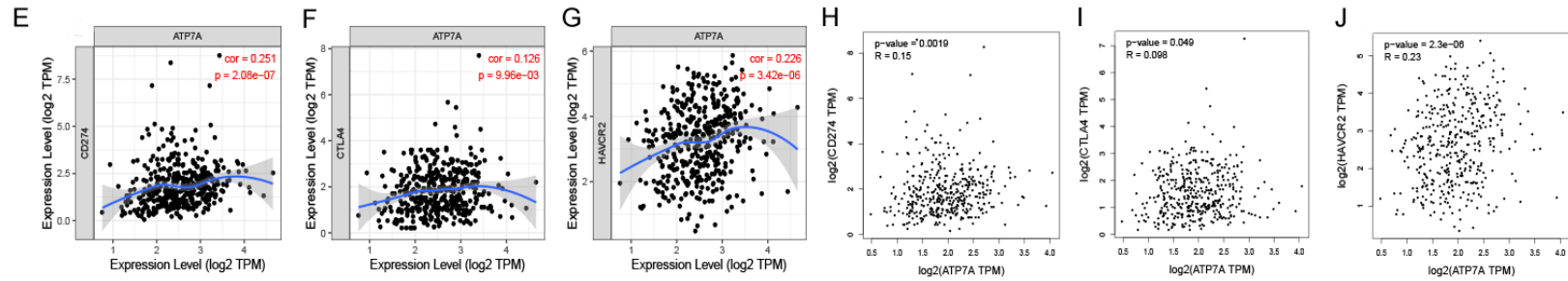


Figure 7. ATP7A expression mediated immune cell infiltration in GC. A. TIMER database was employed to analyze ATP7A levels in 6 immune cell subsets. B. The SCNA of ATP7A was described in B cells, CD8+ T cells, CD4+ T cells, macrophages, neutrophils and DC cells. C. The differential expression of ATP7A in 24 types of immune cells. D. The effect of ATP7A on immune cell surface markers. E-G. The comparison of ATP7A on immune checkpoints CD274, CTLA-4, HAVCR2 by Spearman's correlation analysis. H-J. The relationship between ATP7A and immune checkpoints was described in GEPIA database. Compared with low expression of ATP7A, * $P < 0.05$, ** $P < 0.01$, *** $P < 0.001$.

ATP7A in gastric cancer: biomarker and therapeutic target

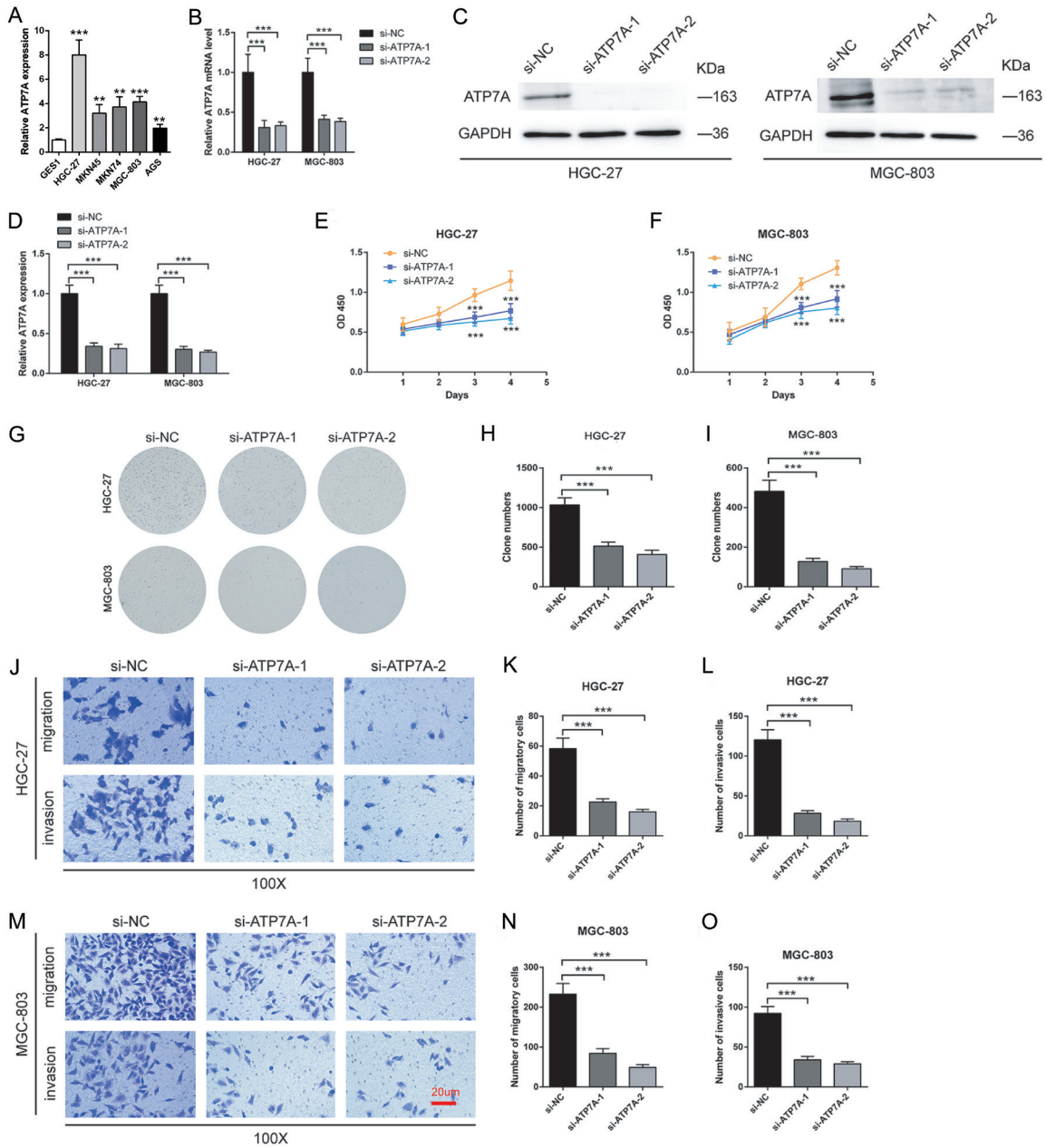


Figure 8. The effects of ATP7A in GC cell growth, colony formation, migration, and invasion. HGC-27 and MGC-803 cells were transfected with ATP7A siRNA-1/-2 (si-ATP7A-1/2) or negative control siRNA (Si-NC). A. Expression of ATP7A in GC cell lines by qPCR. B-D. qPCR and Western blot were used to explore the transfection efficacy of siRNA. E, F. CCK-8 assays were performed to assess cell proliferation after si-ATP7A transfection. G-I. Colony formation assays were conducted in both cell lines. J-O. Transwell assays for cell migration and invasion. Scale bar = 20 μ m. Compared with si-NC, * $P < 0.05$, ** $P < 0.01$, *** $P < 0.001$.

stem cells, and tumor microenvironment (TME) modulation, we hypothesized that ATP7A may regulate GC initiation and progression. To test this hypothesis, we silenced ATP7A in GC cells, and our results demonstrated a significant inhibition of cell proliferation, colony formation, migration, and invasion. Taken together, these

findings suggest that ATP7A could be a crucial target in GC progression and prognosis.

In the TME, immune cell infiltration plays a crucial role, particularly in the context of immunotherapy [34, 35]. Numerous studies have suggested that macrophages in GC tissue can pro-

mote tumor blood vessel formation [36], and M2 macrophages, in particular, drive tumor metastasis and angiogenesis by secreting various cytokines and exerting immunosuppressive effects [37]. The extracellular vesicles of M2 macrophages also contribute to GC progression [38]. Additionally, dendritic cells in the TME have altered metabolic pathways, which impact tumor immunity. These dendritic cells accumulate oxidized lipids, further promoting tumor progression [39]. In this study, we examined the infiltration of immune cells in groups with differential ATP7A expression. We found a positive correlation between ATP7A expression and the infiltration of dendritic cells, T cell subsets (CD8+ and CD4+), B cells, macrophages, and neutrophils. ATP7A expression also influenced immune cell surface markers in GC, particularly CD163, MRC1, IL-10, VISG4, MS4A4A, CD1C, ITGAX, NRP1, and THBD. These findings, in line with previous reports, suggest that immune cell infiltration may play a role in ATP7A-mediated carcinogenesis. The effectiveness of immunotherapy relies on immune cell activity and the expression of immune checkpoints in the TME, especially PD1/PD-L1, CTLA-4, and TIM-3 [40, 41]. Therefore, it is essential to explore the relationship between ATP7A expression and the regulation of these immune checkpoints in GC. Our results revealed significant associations between high ATP7A expression and the levels of PD-L1, CTLA-4, and TIM-3 in GC tissues. Based on these observations, we conclude that ATP7A may influence GC treatment outcomes by mediating immune cell infiltration and checkpoint expression. Further investigations into the complex immune regulatory mechanisms of ATP7A will be the focus of our future studies.

Conclusion

In summary, this is the first study to confirm the overexpression of ATP7A in GC and its association with poor prognosis in patients. We have demonstrated that ATP7A plays a carcinogenic role by promoting cell proliferation, migration, and invasion. However, regarding the immune landscape, we have only analyzed public databases to explore immune cell infiltration and regulatory signaling pathways associated with ATP7A expression. Further verification through experimental studies is required in future work to confirm these findings.

Disclosure of conflict of interest

None.

Address correspondence to: Zhongmei Shi, Department of Laboratory Medicine, Affiliated Hospital of Nantong University, Medical School of Nantong University, No. 20, Xisi Road, Nantong 226001, Jiangsu, China. E-mail: meimei9107@163.com

References

- [1] Bray F, Laversanne M, Sung H, Ferlay J, Siegel RL, Soerjomataram I and Jemal A. Global cancer statistics 2022: GLOBOCAN estimates of incidence and mortality worldwide for 36 cancers in 185 countries. *CA Cancer J Clin* 2024; 74: 229-263.
- [2] Zhu X, Ge B, Wen L, Huang H and Shi X. Analysis of multiple factors influencing the survival of patients with advanced gastric cancer. *Ageing (Albany NY)* 2024; 16: 8541-8551.
- [3] Chen Y, Jia K, Sun Y, Zhang C, Li Y, Zhang L, Chen Z, Zhang J, Hu Y, Yuan J, Zhao X, Li Y, Gong J, Dong B, Zhang X, Li J and Shen L. Predicting response to immunotherapy in gastric cancer via multi-dimensional analyses of the tumour immune microenvironment. *Nat Commun* 2022; 13: 4851.
- [4] Tsvetkov P, Coy S, Petrova B, Dreishpoon M, Verma A, Abdusamad M, Rossen J, Joesch-Cohen L, Humeidi R, Spangler RD, Eaton JK, Frenkel E, Kocak M, Corsello SM, Lutsenko S, Kanarek N, Santagata S and Golub TR. Copper induces cell death by targeting lipoylated TCA cycle proteins. *Science* 2022; 375: 1254-1261.
- [5] Liu H, Bao X, Zeng Z, Liu W and Li M. Analysis of cuproptosis-related genes in prognosis and immune infiltration in grade 4 diffuse gliomas. *Heliyon* 2024; 10: e29212.
- [6] Wang Y, Wang J, Jiang J, Zhang W, Sun L, Ge Q, Li C, Li X, Li X and Shi S. Identification of cuproptosis-related miRNAs in triple-negative breast cancer and analysis of the miRNA-mRNA regulatory network. *Heliyon* 2024; 10: e28242.
- [7] Liu Q, Zhu J, Huang Z, Zhang X and Yang J. Identification of novel cuproptosis-related genes mediating the prognosis and immune microenvironment in cholangiocarcinoma. *Technol Cancer Res Treat* 2024; 23: 15330338241239139.
- [8] Jiang X, Ke J, Jia L, An X, Ma H, Li Z and Yuan W. A novel cuproptosis-related gene signature of prognosis and immune microenvironment in head and neck squamous cell carcinoma cancer. *J Cancer Res Clin Oncol* 2023; 149: 203-218.

ATP7A in gastric cancer: biomarker and therapeutic target

- [9] La Fontaine S, Ackland ML and Mercer JF. Mammalian copper-transporting P-type ATPases, ATP7A and ATP7B: emerging roles. *Int J Biochem Cell Biol* 2010; 42: 206-209.
- [10] Petruzzelli R and Polishchuk RS. Activity and trafficking of copper-transporting ATPases in tumor development and defense against platinum-based drugs. *Cells* 2019; 8: 1080.
- [11] Shao K, Shen H, Chen X, Shao Z, Liu Y, Wang Y, Chen H and Wu X. Copper transporter gene ATP7A: a predictive biomarker for immunotherapy and targeted therapy in hepatocellular carcinoma. *Int Immunopharmacol* 2023; 114: 109518.
- [12] Li ZH, Lu X, Li SW, Chen JT and Jia J. Expression of ATP7A in esophageal squamous cell carcinoma (ESCC) and its clinical significance. *Int J Clin Exp Pathol* 2019; 12: 3521-3525.
- [13] Tomczak K, Czerwinska P and Wiznerowicz M. The Cancer Genome Atlas (TCGA): an immeasurable source of knowledge. *Contemp Oncol (Pozn)* 2015; 19: A68-77.
- [14] Yin F, Yi S, Wei L, Zhao B, Li J, Cai X, Dong C and Liu X. Microarray-based identification of genes associated with prognosis and drug resistance in ovarian cancer. *J Cell Biochem* 2019; 120: 6057-6070.
- [15] Chandrashekar DS, Karthikeyan SK, Korla PK, Patel H, Shovon AR, Athar M, Netto GJ, Qin ZS, Kumar S, Manne U, Creighton CJ and Varambally S. UALCAN: an update to the integrated cancer data analysis platform. *Neoplasia* 2022; 25: 18-27.
- [16] Uhlen M, Fagerberg L, Hallstrom BM, Lindskog C, Oksvold P, Mardinoglu A, Sivertsson A, Kampf C, Sjostedt E, Asplund A, Olsson I, Edlund K, Lundberg E, Navani S, Szgyarto CA, Odeberg J, Djureinovic D, Takanen JO, Hober S, Alm T, Edqvist PH, Berling H, Tegel H, Mulder J, Rockberg J, Nilsson P, Schwenk JM, Hamsten M, von Feilitzen K, Forsberg M, Persson L, Johansson F, Zwahlen M, von Heijne G, Nielsen J and Ponten F. Proteomics. Tissue-based map of the human proteome. *Science* 2015; 347: 1260419.
- [17] Szklarczyk D, Gable AL, Lyon D, Junge A, Wyder S, Huerta-Cepas J, Simonovic M, Doncheva NT, Morris JH, Bork P, Jensen LJ and Mering CV. STRING v11: protein-protein association networks with increased coverage, supporting functional discovery in genome-wide experimental datasets. *Nucleic Acids Res* 2019; 47: D607-D613.
- [18] Li T, Fan J, Wang B, Traugh N, Chen Q, Liu JS, Li B and Liu XS. TIMER: a web server for comprehensive analysis of tumor-infiltrating immune cells. *Cancer Res* 2017; 77: e108-e110.
- [19] Yu G, Wang LG, Han Y and He QY. clusterProfiler: an R package for comparing biological themes among gene clusters. *OMICS* 2012; 16: 284-287.
- [20] Subramanian A, Tamayo P, Mootha VK, Mukherjee S, Ebert BL, Gillette MA, Paulovich A, Pomeroy SL, Golub TR, Lander ES and Mesirov JP. Gene set enrichment analysis: a knowledge-based approach for interpreting genome-wide expression profiles. *Proc Natl Acad Sci U S A* 2005; 102: 15545-15550.
- [21] Liberzon A, Birger C, Thorvaldsdóttir H, Ghandi M, Mesirov JP and Tamayo P. The molecular signatures database (MSigDB) hallmark gene set collection. *Cell Syst* 2015; 1: 417-425.
- [22] Hanzelmann S, Castelo R and Guinney J. GSVA: gene set variation analysis for microarray and RNA-seq data. *BMC Bioinformatics* 2013; 14: 7.
- [23] Bindea G, Mlecnik B, Tosolini M, Kirilovsky A, Waldner M, Obenauf AC, Angell H, Fredriksen T, Lafontaine L, Berger A, Bruneval P, Fridman WH, Becker C, Pages F, Speicher MR, Trajanoski Z and Galon J. Spatiotemporal dynamics of intratumoral immune cells reveal the immune landscape in human cancer. *Immunity* 2013; 39: 782-795.
- [24] Tang Z, Li C, Kang B, Gao G, Li C and Zhang Z. GEPIA: a web server for cancer and normal gene expression profiling and interactive analyses. *Nucleic Acids Res* 2017; 45: W98-W102.
- [25] Lanczky A and Györfy B. Web-based survival analysis tool tailored for medical research (KMplot): development and implementation. *J Med Internet Res* 2021; 23: e27633.
- [26] Robin X, Turck N, Hainard A, Tiberti N, Lisacek F, Sanchez JC and Muller M. pROC: an open-source package for R and S+ to analyze and compare ROC curves. *BMC Bioinformatics* 2011; 12: 77.
- [27] Polishchuk R and Lutsenko S. Golgi in copper homeostasis: a view from the membrane trafficking field. *Histochem Cell Biol* 2013; 140: 285-295.
- [28] Horn N and Wittung-Stafshede P. ATP7A-regulated enzyme metalation and trafficking in the menkes disease puzzle. *Biomedicines* 2021; 9: 391.
- [29] Moller LB, Mogensen M, Weaver DD and Pedersen PA. Occipital horn syndrome as a result of splice site mutations in ATP7A. No activity of ATP7A splice variants missing Exon 10 or Exon 15. *Front Mol Neurosci* 2021; 14: 532291.
- [30] Kennerson ML, Nicholson GA, Kaler SG, Kowalski B, Mercer JF, Tang J, Llanos RM, Chu S, Takata RI, Speck-Martins CE, Baets J, Almeida-Souza L, Fischer D, Timmerman V, Taylor PE, Scherer SS, Ferguson TA, Bird TD, De Jonghe P, Feely SM, Shy ME and Garbern JY. Missense mutations in the copper transporter gene ATP7A cause X-linked distal hereditary motor

ATP7A in gastric cancer: biomarker and therapeutic target

- neuropathy. *Am J Hum Genet* 2010; 86: 343-352.
- [31] Samimi G, Varki NM, Wilczynski S, Safaei R, Alberts DS and Howell SB. Increase in expression of the copper transporter ATP7A during platinum drug-based treatment is associated with poor survival in ovarian cancer patients. *Clin Cancer Res* 2003; 9: 5853-5859.
- [32] Li YQ, Yin JY, Liu ZQ and Li XP. Copper efflux transporters ATP7A and ATP7B: novel biomarkers for platinum drug resistance and targets for therapy. *IUBMB Life* 2018; 70: 183-191.
- [33] Chatterjee S and Sil PC. Targeting the cross-talks of Wnt pathway with Hedgehog and Notch for cancer therapy. *Pharmacol Res* 2019; 142: 251-261.
- [34] Lu J, Xu Y, Wu Y, Huang XY, Xie JW, Wang JB, Lin JX, Li P, Zheng CH, Huang AM and Huang CM. Tumor-infiltrating CD8+ T cells combined with tumor-associated CD68+ macrophages predict postoperative prognosis and adjuvant chemotherapy benefit in resected gastric cancer. *BMC Cancer* 2019; 19: 920.
- [35] Zhang H, Liu H, Shen Z, Lin C, Wang X, Qin J, Qin X, Xu J and Sun Y. Tumor-infiltrating neutrophils is prognostic and predictive for postoperative adjuvant chemotherapy benefit in patients with gastric cancer. *Ann Surg* 2018; 267: 311-318.
- [36] Li H, Wang JS, Mu LJ, Shan KS, Li LP and Zhou YB. Promotion of Sema4D expression by tumor-associated macrophages: significance in gastric carcinoma. *World J Gastroenterol* 2018; 24: 593-601.
- [37] Yamaguchi T, Fushida S, Yamamoto Y, Tsukada T, Kinoshita J, Oyama K, Miyashita T, Tajima H, Ninomiya I, Munesue S, Harashima A, Harada S, Yamamoto H and Ohta T. Tumor-associated macrophages of the M2 phenotype contribute to progression in gastric cancer with peritoneal dissemination. *Gastric Cancer* 2016; 19: 1052-1065.
- [38] Zheng P, Chen L, Yuan X, Luo Q, Liu Y, Xie G, Ma Y and Shen L. Exosomal transfer of tumor-associated macrophage-derived miR-21 confers cisplatin resistance in gastric cancer cells. *J Exp Clin Cancer Res* 2017; 36: 53.
- [39] Cubillos-Ruiz JR, Silberman PC, Rutkowski MR, Chopra S, Perales-Puchalt A, Song M, Zhang S, Bettigole SE, Gupta D, Holcomb K, Ellenson LH, Caputo T, Lee AH, Conejo-Garcia JR and Glimcher LH. ER stress sensor XBP1 controls anti-tumor immunity by disrupting dendritic cell homeostasis. *Cell* 2015; 161: 1527-1538.
- [40] Chae YK, Arya A, Iams W, Cruz MR, Chandra S, Choi J and Giles F. Current landscape and future of dual anti-CTLA4 and PD-1/PD-L1 blockade immunotherapy in cancer; lessons learned from clinical trials with melanoma and non-small cell lung cancer (NSCLC). *J Immunother Cancer* 2018; 6: 39.
- [41] Zeidan AM, Komrokji RS and Brunner AM. TIM-3 pathway dysregulation and targeting in cancer. *Expert Rev Anticancer Ther* 2021; 21: 523-534.